Biophysics of selectin–ligand interactions in inflammation and cancer

2011 Phys. Biol. 8 015013

(http://iopscience.iop.org/1478-3975/8/1/015013)

Phys. Biol. **8** (2011) 015013 (14pp) doi:10.1088/1478-3975/8/1/015013

Biophysics of selectin–ligand interactions in inflammation and cancer

Luthur Siu-Lun Cheung[1,4], Phrabha S Raman[1,4], Eric M Balzer[1,2,3], Denis Wirtz[1,2,3] and Konstantinos Konstantopoulos[1,2,3,5]

[1] Department of Chemical and Biomolecular Engineering, The Johns Hopkins University, Baltimore, MD 21218, USA
[2] NCI PS-OC Johns Hopkins Engineering in Oncology Center, The Johns Hopkins University, Baltimore, MD 21218, USA
[3] Institute for NanoBioTechnology, The Johns Hopkins University, Baltimore, MD 21218, USA

E-mail: kkonsta1@jhu.edu

Received 21 September 2010
Accepted for publication 15 November 2010
Published 7 February 2011
Online at stacks.iop.org/PhysBio/8/015013

Abstract
Selectins (L-, E- and P-selectin) are calcium-dependent transmembrane glycoproteins that are expressed on the surface of circulating leukocytes, activated platelets, and inflamed endothelial cells. Selectins bind predominantly to sialofucosylated glycoproteins and glycolipids (E-selectin only) present on the surface of apposing cells, and mediate transient adhesive interactions pertinent to inflammation and cancer metastasis. The rapid turnover of selectin–ligand bonds, due to their fast on- and off-rates along with their remarkably high tensile strengths, enables them to mediate cell tethering and rolling in shear flow. This paper presents the current body of knowledge regarding the role of selectins in inflammation and cancer metastasis, and discusses experimental methodologies and mathematical models used to resolve the biophysics of selectin-mediated cell adhesion. Understanding the biochemistry and biomechanics of selectin–ligand interactions pertinent to inflammatory disorders and cancer metastasis may provide insights for developing promising therapies and/or diagnostic tools to combat these disorders.

Introduction

Cell adhesion in shear flow is instrumental in diverse biological processes including inflammation and cancer metastasis. Leukocyte recruitment to sites of inflammation or infection is mediated by highly specific receptor–ligand interactions that allow leukocytes to first tether and roll on activated endothelium under hydrodynamic shear and then firmly adhere prior to their extravasation into the tissue space. During the metastatic process, tumor cells invade the surrounding tissues to reach and penetrate the vascular endothelium. Once they enter the circulatory system, these rogue cancerous cells, referred to as circulating tumor cells (CTCs), are subjected to shear forces and immunological stresses, which may affect their ability to metastasize. Only tumor cells uniquely fit to overcome or even exploit the effects of hemodynamic forces and immunosurveillance will adhere to the vascular endothelium of distant organs, extravasate and successfully colonize these sites. Thus, only a tiny fraction of CTCs is capable of establishing secondary colonies (Fidler *et al* 2002); most CTCs die or remain dormant. Understanding the molecular and biophysical underpinnings of CTC adhesion to host cells in shear flow may provide guidelines for developing promising anti-metastatic therapies when initiated early in the course of disease progression.

Accumulating evidence suggests that the adhesive interactions of CTCs with host cells, such as platelets, leukocytes and endothelial cells, modulate their extravasation from the vasculature, and thus the development of secondary metastatic foci. For instance, CTCs may escape immune surveillance and promote their extravasation from the circulatory system by co-opting platelets. Direct evidence for the involvement of platelets in the facilitation of hematogenous dissemination of tumor cells stems from studies showing inhibition of metastasis by either pharmacological (Gasic *et al*

[4] Both authors contributed equally to this work.
[5] Author to whom any correspondence should be addressed.

1968, Karpatkin *et al* 1988) or genetic depletion (Camerer *et al* 2004) of platelets, and the restoration of metastatic potential by platelet infusion in a mouse model (Karpatkin *et al* 1988). It is believed among others that platelets, by forming heterotypic adhesive clusters with CTCs (Borsig *et al* 2001, 2002), mask and protect CTCs from immune-mediated mechanisms of clearance (Nieswandt *et al* 1999, Palumbo *et al* 2005). Alternatively, platelets may potentiate tumor cell adhesion to the vessel wall via a platelet bridging mechanism, in which platelets adherent to an endothelial-bound tumor cell capture free-flowing CTCs that subsequently attach to the vessel wall downstream or next to the already adherent cell (Burdick and Konstantopoulos 2004). Platelets may also secrete an array of bioactive compounds, such as vascular endothelial growth factor (VEGF) at points of attachment to endothelium, thereby promoting vascular hyperpermeability and extravasation (Nash *et al* 2002). Once tumor cells have exited the circulation, factors released from activated platelets are capable of inducing angiogenesis and stimulating growth at the metastatic site (Pinedo *et al* 1998). CTCs can also hijack polymorphonuclear leukocytes (PMNs) for arrest in the endothelium of distant organs. PMN-facilitated CTC arrest under hydrodynamic shear involves initial PMN tethering on the endothelium and subsequent capture of free-flowing tumor cells by tethered PMNs. CTCs may also masquerade as immune cells and directly bind to vascular endothelium in a manner analogous to leukocyte recruitment, which involves tethering, rolling and firm adhesion (Burdick *et al* 2003, Burdick and Konstantopoulos 2004). Selectins mediate the initial tethering and rolling events during leukocyte accumulation to sites of inflammation. Similarly, selectins facilitate cancer metastasis (Borsig *et al* 2001, 2002, Mannori *et al* 1997) and tumor cell arrest in the microvasculature by mediating the specific interactions between selectin-expressing host cells and ligands on tumor cells (Burdick and Konstantopoulos 2004, Burdick *et al* 2003, Jadhav *et al* 2001, Jadhav and Konstantopoulos 2002, McCarty *et al* 2000, 2002). Indeed, a variety of tumor cells, such as colon and pancreatic carcinoma cells, express sialofucosylated molecules that are recognized by selectins (Mannori *et al* 1995, Park *et al* 2003, Satomura *et al* 1991).

The adhesion of leukocytes and CTCs to endothelial cells involves highly regulated molecular events such as selectin–ligand interactions that rely on the local circulatory hemodynamics and the micromechanical and kinetic properties of participating adhesive molecular constituents. Fluid shear generated by blood flow, on one hand, induces collisions among free-flowing cells as well as between free-flowing cells and the vessel wall, thereby increasing the encounter rate between membrane-bound receptors and their cognate ligands. On the other hand, fluid shear reduces the cell–cell contact duration, and exerts tensile forces tending to disrupt the receptor–ligand bonds that are responsible for cell adhesion. Particle size and compliance also modulate the extent of cell adhesion in shear flow (Jadhav *et al* 2005, Pawar *et al* 2008). The ability to predict cell–cell binding will be vital to the optimization of design parameters, such as site density, affinity and tensile strength of targeted receptor–ligand interactions, for developing effective targeted drug delivery strategies to combat inflammatory disorders and cancer metastasis.

In this paper we discuss the critical roles of selectins and newly discovered functional selectin ligands in cancer metastasis. We proceed with a description of experimental techniques and mathematical models used to resolve the biophysics of selectin-mediated cell adhesion pertinent to inflammation. These biophysical/mathematical approaches can be readily applied to resolve the selectin–ligand binding interactions in the area of cancer metastasis. Understanding the biochemical and biophysical underpinnings of selectin–ligand interactions pertinent to inflammation and cancer metastasis may provide insights for combating these disorders.

Selectins and selectin ligands on host cells and tumor cells

Selectins are calcium-dependent transmembrane glycoproteins that recognize specific glycoconjugates on apposing cell surfaces (Kansas 1996, Varki 1997), and play pivotal roles in the cell–cell interactions pertinent to inflammation and cancer metastasis. All three known members of the selectin family (L-, E-, and P-selectin) share a similar cassette structure: an N-terminal, calcium-dependent lectin domain, an epidermal-growth-factor (EGF)-like domain, a variable number of consensus repeat units (2, 6, and 9 for L-, E-, and P-selectin, respectively), a transmembrane domain (TM) and an intracellular cytoplasmic tail (cyto). Though they share common elements, their tissue distribution and binding kinetics are quite different, reflecting their divergent roles in various pathophysiological processes.

L-selectin (CD62L) is constitutively expressed on the surface of almost all types of leukocytes but gets rapidly shed upon cell activation with cytokines, chemokines, or formyl peptides. Expression of P-selectin (CD62P) on endothelium and platelet surfaces is inducible. E-selectin (CD62E) expression is induced on vascular endothelial cells and requires *de novo* mRNA and protein synthesis. Maximal level of E-selectin expression typically occurs 4–6 h after activation with inflammatory stimuli, such as interleukin-1, tumor necrosis factor-alpha or endotoxin *in vitro*. P-selectin is stored preformed in the Weibel–Palade bodies of endothelial cells and alpha-granules of platelets, and is rapidly mobilized to the plasma membrane upon activation with agonists like histamine or thrombin. However, P-selectin expression on vascular endothelium may also be regulated at the transcriptional level after stimulation with cytokines such as interleukin-4 or oncostatin M (Yao *et al* 1996).

Selectins, like all C-type lectins, bind to carbohydrate ligands in a calcium-dependent manner. Detailed studies involving site-directed mutagenesis, domain swapping, and antibody inhibition have revealed that carbohydrate ligands bind to the lectin domain on a shallow region that overlaps a single calcium coordination site opposite where the EGF domain is located (Kansas 1996, Varki 1997). Evidence also suggests that the EGF domain and the short consensus repeat domains not only contribute to ligand specificity but also confer unique kinetic and mechanical properties on

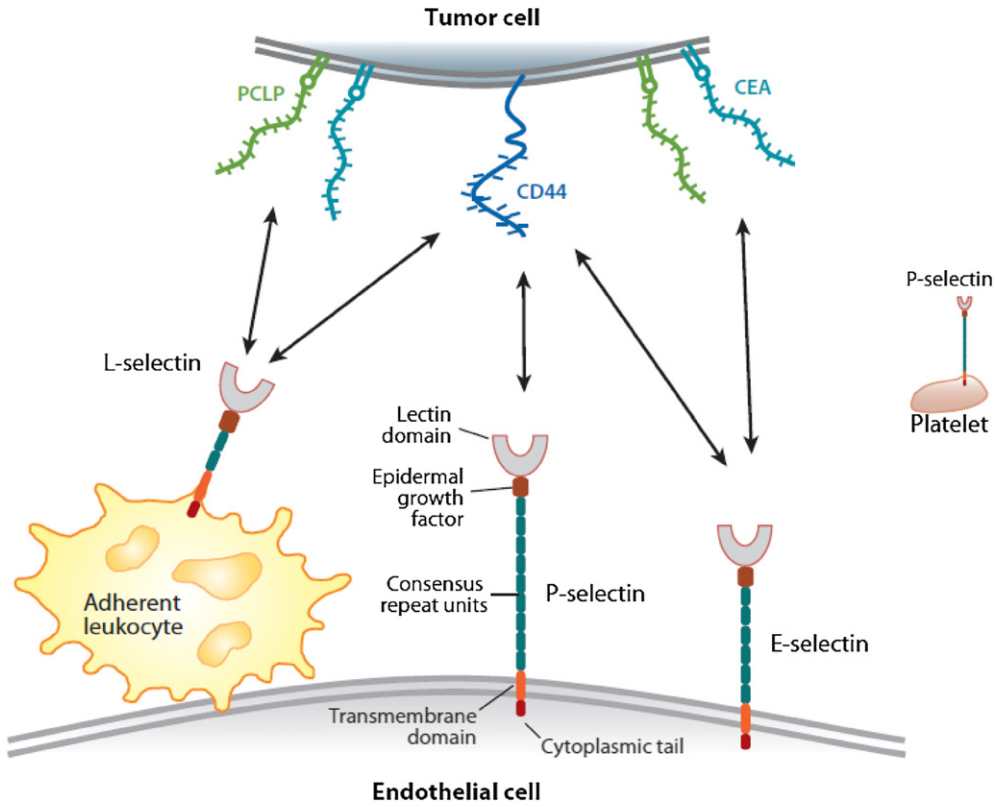

Figure 1. Schematic diagram of selectin–ligand interactions between tumor cells and host vascular cells. CD44 on free-flowing tumor cells binds to P-selectin on activated endothelial cells or platelets, whereas CD44, CEA, and PCLP mediate E-selectin-dependent tumor cell adhesion to endothelial cells. CD44, CEA, and PCLP also bind to L-selectin expressed by leukocytes. Adopted from Konstantopoulos and Thomas (2009).

each selectin when binding to its ligand (Patel *et al* 1995b). All selectins recognize the tetrasaccharide sialyl Lewis x (sLe^x; NeuAc α2,3 Gal β1,4 [Fuc α1,3] GlcNAc-R) and its isomer sialyl Lewis a (sLe^a; NeuAc α2,3 Gal β1,3 [Fuc α1,4] GlcNAc-R) (Kansas 1996, Varki 1997). sLe^x is a terminal component of glycans attached to glycoproteins and glycolipids on most circulating leukocytes and some endothelial cells. In contrast, sLe^a is expressed on some tumor cells but not on normal leukocytes. The affinity of selectins for isolated monovalent sLe^x and sLe^a oligosaccharides is very low (Nicholson *et al* 1998, Poppe *et al* 1997). Thus, neither expression of the sLe^x nor the sLe^a groups correlate with the properties of endogenous selectin ligands on cellular targets *per se*. Instead, sLe^x or related structures are part of more extensive binding determinants. Selectins can also recognize other classes of molecules, namely non-sialylated or non-fucosylated molecules such as heparan sulfate glycosaminoglycans, sulfated glycolipids such as sulfatides, and sulfoglucuronosyl glycosphingolipids (Varki 1997).

High affinity ligands for P- and L-selectin have been identified (figure 1). P-selectin binds to the amino terminus of P-selectin glycoprotein ligand-1 (PSGL-1; CD162), which is expressed on nearly all blood leukocytes, human hematopoietic progenitor cells (McEver and Cummings 1997a), and to a much lesser extent on blood platelets (Frenette *et al* 2000). The extracellular domain of PSGL-1 (~60 nm long) has the hallmarks of a mucin, since it is rich in serines, threonines and prolines, and includes 16 decameric repeats (McEver and Cummings 1997b). High affinity binding of PSGL-1 to P- and L-selectin requires three clustered tyrosine sulfate residues, adjacent peptide components, and fucose and sialic acid residues on an optimally positioned short core-2 O-glycan within the anionic amino-terminal region of PSGL-1 (Leppanen *et al* 2000). Crystallographic studies reveal a patch of positive electrostatic potential on P-selectin designed to engage the tyrosine sulfate residues and increase the binding affinity (Somers *et al* 2000). Although PSGL-1 is recognized by all three selectins (Hanley *et al* 2004, Patel *et al* 1995a), it serves as functional ligand only for P- and L-selectin, since selective removal or blockade of PSGL-1 on intact human leukocytes nearly abrogates their binding to P- and L-selectin (Patel *et al* 1995b, Walcheck *et al* 1996). In contrast, PSGL-1 appears dispensable for E-selectin-dependent binding of human PMNs (Nimrichter *et al* 2008).

L-selectin also binds to a series of mucin-type glycoproteins such as CD34, podocalyxin-like protein (PCLP) and MadCAM-1 that contain O-linked glycans in which the sLe^x determinant is present and further substituted with a sulfate ester on the 6-hydroxyl group of the GlcNAc (NeuAc a2,3 Gal ß1,4 [Fuc a1,3] SO36-GlcNAc; 6-sulfo-sLe^x) and/or Gal (NeuAc a2,3 SO36-Gal ß1,4 [Fuc a1,3] GlcNAc; 6′-sulfo-sLe^x) residues (Rosen 2004). The sulfate residue on GlcNAc is required for high-affinity L-selectin-dependent binding, while the contribution of Gal-6-sulfation is controversial (Rosen 2004).

Although E-selectin binds to PSGL-1 (Hanley *et al* 2004), accumulating evidence supports the concept that sialylated fucosylated glycolipids on human PMNs represent the physiologically relevant E-selectin ligands (Alon *et al* 1995a, Burdick *et al* 2001, Nimrichter *et al* 2008). Also, L-selectin itself has been reported as a high-affinity ligand for E-selectin. Direct evidence for this interaction was provided in affinity isolation experiments with E-selectin-Ig, which also documented that the binding was dependent on sialic acid on L-selectin (Zollner *et al* 1997). Although the inhibitory effects of anti-L-selectin mAbs on PMN binding to E-selectin-coated surfaces were initially ascribed to the blockade of the so-called secondary tethering mediated by L-selectin on free-flowing cell and L-selectin ligands on already adherent leukocytes (Alon *et al* 1996), it has been reported that antibody blockade interferes with primary interactions between L- and E-selectin (Zollner *et al* 1997).

A variety of tumor cells, including colon and pancreatic carcinoma cells, express sialofucosylated molecules (Mannori *et al* 1995, Park *et al* 2003, Satomura *et al* 1991, Kannagi 1997) that are recognized by selectins. However, the characterization of selectin ligands on tumor cells beyond general classifications (i.e. sialofucosylated mucin-like glycoproteins) has recently begun to emerge. As described by Varki (1997), distinctions must be drawn between molecules that can bind to selectins under static conditions *in vitro* and those (i.e. the functional ligands) that actually interact with selectins *in vivo*. To this end, a functional selectin ligand should fulfill certain criteria: it should be expressed in the right place and at the right time, the ligand should bind with some selectivity and relatively high affinity, and selective removal or absence of the ligand should prevent cell adhesive interactions. CD44 variant isoforms, CD44v, have been identified as P-selectin ligands that fit the aforementioned criteria (Napier *et al* 2007) (figure 1). CD44 proteins are type I transmembrane molecules encoded by a single gene that comprises at least 20 exons. Exons 1–5, 16–18 and 20 are spliced together to form the smallest CD44 transcript, known as standard isoform (CD44s). However, CD44s displays a rather low affinity for P-selectin (Hanley *et al* 2006). It is believed that the structural biology of CD44 is such that splicing of variant exons into CD44 by metastatic tumor cells extends its molecular length and inserts additional sites for glycosylation, thereby transforming CD44v into a mucin-like sialofucosylated glycoprotein capable of functioning as an efficient P-selectin ligand. CD44v also serves as an ancillary L-selectin ligand by stabilizing L-selectin-dependent tumor cell rolling (Napier *et al* 2007). In contrast, CD44 appears dispensable for E-selectin-dependent binding (Napier *et al* 2007). Of note, CD44v overexpressing in certain types of cancer confers resistance to apoptosis, metastatic potential *in vivo* and leads to prognosis (Harada *et al* 2001, Wielenga *et al* 1993).

Carcinoembryonic antigen (CEA) was recently shown to possess L- and E-, but not P-, selectin ligand activity on colon carcinoma cells (Thomas *et al* 2008a) (figure 1). Most importantly, CEA and CD44v cooperate to mediate colon carcinoma cell adhesion to L- and E-selectin in shear flow (Thomas *et al* 2008a). Interestingly, CEA is expressed in a number of tumors of epithelial origin including colorectal carcinoma, lung adenocarcinoma and mucinous ovarian carcinoma, and has been reported to promote the metastatic potential of colon carcinoma cells (Hashino *et al* 1994, Minami *et al* 2001). PCLP was also found to support L- and E-, but not P-selectin-dependent tethering and rolling of metastatic colon carcinoma cells in shear flow (Thomas *et al* 2009a) (figure 1). The selectin-binding determinants on PCLP expressed by tumor cells are non-sulfated (MECA-79-negative) sialofucosylated structures displayed on O-linked glycans (Thomas *et al* 2009a, 2009b), distinct from the MECA-79-reactive O-glycans expressed by high endothelial venules, which possess L-selectin ligand activity. Of note, PCLP is expressed by a number of metastatic tumor cells such as colon and breast carcinoma (Somasiri *et al* 2004, Thomas *et al* 2009a). PCLP overexpression has been reported as an independent predictor of breast cancer progression (Somasiri *et al* 2004).

The role of selectins in cancer metastasis

Mounting evidence suggests that selectins facilitate the hematogenous dissemination of tumor cells and their arrest in the microvasculature by mediating specific interactions between selectin-expressing host cells and ligands on tumor cells. The most direct evidence for the involvement of P-selectin in the metastatic process is the marked inhibition of metastasis in P-selectin-deficient mice compared to wild-type (wt) controls in a colon carcinoma cell model (Borsig *et al* 2001, Kim *et al* 1998). Microscopic observations of tumor cells arrested in the lungs of wt mice reveal the presence of a dense coat of platelets surrounding the colon carcinoma cells that is diminished in P-selectin-deficient mice (Borsig *et al* 2001). Moreover, the initial seeding and subsequent lodging of metastatic cells in target organs was mitigated in P-selectin-knockout mice compared to wt controls (Borsig *et al* 2001, Kim *et al* 1998). Although these observations suggest that platelet P-selectin plays a critical role not only in colon carcinoma-platelet adhesion but also in the facilitation of metastasis, they cannot rule out an additional role for endothelial P-selectin that could potentially tether tumor cells and mediate their extravasation from the vasculature. *In vivo* studies also disclose the role of L-selectin in cancer metastasis (Borsig *et al* 2002). It is believed that tumor cells can form multicellular complexes with platelets and leukocytes (via an L-selectin-dependent mechanism) (Jadhav *et al* 2001, Jadhav and Konstantopoulos 2002), which can then arrest in the microvasculature of distant organs, and eventually extravasate and establish metastatic colonies. Selectins can thus act synergistically to facilitate tumor cell–host cell interactions and cancer metastasis. To date, the cooperative effects of P- and L-selectin on cancer metastasis have been demonstrated *in vivo* (Borsig *et al* 2002). Interestingly, leukocyte L-selectin can also enhance metastasis by interacting with endothelial L-selectin ligands induced adjacent to established intravascular colon carcinoma cell emboli (Laubli *et al* 2006). Endothelial E-selectin has been shown to support metastatic spread

in vivo (Mannori *et al* 1997). Since selectins recognize sLe^x- and/or sLe^a-decorated glycoproteins such as CD44v, CEA and PCLP, and over-expression of these moieties on tumor cells correlates with poor prognosis and tumor progression (Kannagi 1997, Konstantopoulos and Thomas 2009, Thomas *et al* 2009b), it appears that selectin-mediated adhesion to these sialofucosylated target molecules on tumor cells is an important determinant for metastatic spread.

The ability of selectin–ligand bonds to initiate tethering and rolling in shear flow is dictated by their micromechanical and kinetic properties, and their responses to external force. Below, we review quantitative models used to resolve the biophysics of receptor–ligand interactions.

Mathematical models of two-dimensional (2D) receptor–ligand binding affinity

Several techniques, such as surface plasmon resonance and radio-immunoassays, that have been developed to study receptor–ligand binding kinetics require at least one molecule present in solution, which limits their application to the measurement of three-dimensional (3D) binding constants. Yet, cell adhesive interactions are mediated by the binding of receptors to ligands, which are anchored on apposing cell membrane surfaces. Consequently, the motion of both molecules is restricted to 2D (Piper *et al* 1998). Not only the binding mechanism is different but also their respective on-rates have different units (M^{-1} s^{-1} in 3D and μm^2 s^{-1} in 2D). Even though 3D kinetic rates have been extensively reported in the literature, they are inadequate to describe the 2D kinetics of cell–cell adhesive interactions.

Sophisticated biophysical assays have been developed to quantify the 2D receptor–ligand binding kinetics. In the widely used micropipette aspiration assay (Evans *et al* 1991), a red blood cell, serving as a picoforce transducer, coated with a low density of the adhesion receptor of interest is held at a fixed position by a micropipette. Also held by a second micropipette, a cell (PMN) or a ligand-bearing bead is translated to contact the RBC by precision-piezo displacements for prescribed durations of time, and then retracted from the contact position at defined pulling velocities. The deformation of the RBC induced by the receptor–ligand bond is recorded using a video-enhanced microscope. The bond rupture force is readily calculated by multiplying the total extension of RBC with the stiffness of membrane transducer at the moment of bond failure (Evans *et al* 1991, 1995). In addition to measuring force-dependent 2D off-rates, the micropipette aspiration assay can also be used to quantify the 2D affinity constant, $A_c K_a{}^0$, of receptor–ligand bonds (Huang *et al* 2010, Chesla *et al* 1998), as described below.

In this assay, the small contact zone between the target cell (or ligand-bearing bead) and the receptor-coated RBC along with the low site density of adhesion molecules dictate that receptor–ligand binding occurs as a random event, even though all experimental conditions can be kept identical including contact area (A_c), contact duration (t), surface density of receptors (m_r) and ligands (m_l). Hence, the probabilistic model, rather than the deterministic model, is more suitable for this scenario (Chesla *et al* 1998, McQuarrie *et al* 1964).

For a 1-step reversible kinetic system involving v_r receptors (R) binding to v_l ligands (L) to produce v_b bonds (B), its reaction equation is given by

$$v_r R + v_l L \underset{k_r^0}{\overset{k_f^0}{\rightleftharpoons}} v_b B, \tag{1}$$

where k_f^0 and k_r^0 represent the unstressed on- and off-rates, respectively. The rates of change of the probability components (dp_n/dt) are defined as (Chesla *et al* 1998)

$$\begin{aligned}\frac{dp_n}{dt} &= (n+1)^{v_b}\frac{k_r^0}{A_c^{v_b-1}}p_{n+1}\\ &-\left[\left(A_c m_r - \frac{v_r}{v_b}n\right)^{v_r}\left(A_c m_l - \frac{v_l}{v_b}n\right)^{v_l}\frac{k_f^0}{A_c^{v_r+v_l-1}} + n^{v_b}\frac{k_r^0}{A_c^{v_b-1}}\right]p_n\\ &+\left[A_c m_r - \frac{v_r}{v_b}(n-1)\right]^{v_r}\left[A_c m_l - \frac{v_l}{v_b}(n-1)\right]^{v_l}\frac{k_f^0}{A_c^{v_r+v_l-1}}p_{n-1}\end{aligned} \tag{2a}$$

where the first term on the right-hand side of equation (2*a*) represents the probability of $(n+1)$ bonds losing one bond during time t; the second and third terms represent the probability of n bonds adding one or losing one during time t, respectively; and the last term represents the probability of $(n-1)$ adding one bond during time t.

Assuming that the formation of a small number of receptor–ligand bonds will have no appreciable effect on the availability of unbound receptors and ligands inside the contact area, equation (2*a*) can be simplified by neglecting the n and $(n-1)$ terms in $[A_c m_j - (v_j/v_b)n]$ and $[A_c m_j - (v_j/v_b)(n-1)]$ (subscript $j = r$ or l) as given by equation (2*b*) (Chesla *et al* 1998):

$$\begin{aligned}\frac{dp_n}{dt} &= (n+1)^{v_b}\frac{k_r^0}{A_c^{v_b-1}}p_{n+1}\\ &-\left[(A_c m_r)^{v_r}(A_c m_l)^{v_l}\frac{k_f^0}{A_c^{v_r+v_l-1}} + n^{v_b}\frac{k_r^0}{A_c^{v_b-1}}\right]p_n\\ &+(A_c m_r)^{v_r}(A_c m_l)^{v_l}\frac{k_f^0}{A_c^{v_r+v_l-1}}p_{n-1}.\end{aligned} \tag{2b}$$

The solution of equation (2*b*) for the special case, $v_r = v_l = v_b = 1$, is of the form of the Poisson distribution (Chesla *et al* 1998, Long *et al* 1999):

$$P_n(t) = \frac{\langle n\rangle^n}{n!}\exp(-\langle n\rangle) \tag{3}$$

where $\langle n\rangle$ is the average number of bonds at time t given by

$$\langle n\rangle = A_c m_r^{v_r} m_l^{v_l} K_a^0\left[1-\exp\left(-k_r^0 t\right)\right]. \tag{4}$$

Equations (3) and (4) will deviate significantly from the exact solution when the numbers of available receptors and ligands are similar (i.e. $m_r \approx m_l$). The comparison between the approximated solution and exact solution against the ratio of receptor to ligand site densities has been discussed in the literature (Chesla *et al* 1998). The analysis reveals that

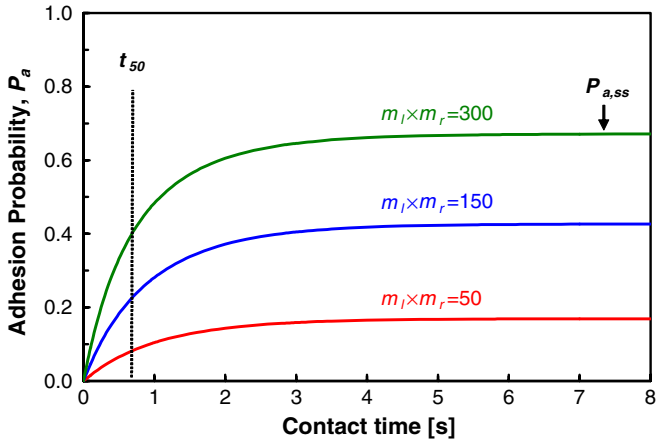

Figure 2. Estimation of the 2D binding kinetics by plotting the adhesion probability as a function of contact duration time for different receptor–ligand site densities ($m_r \times m_l$). The 2D binding affinity $A_c K_a^0$ is estimated from the steady-state value of the adhesion probability ($P_{a,\mathrm{ss}}$) using equation (6). The unstressed dissociation rate k_r^0 is determined from the half-time (t_{50}) using equation (7).

the Poisson distribution given by equation (3) is in excellent agreement with the exact solution if the ratio $A_c m_{\min}/\langle n \rangle$ is >10.

In most chemical reactions, the concentration of the product is proportional to the reaction time until the system reaches equilibrium. Similar reaction characteristics have been observed for receptor–ligand-mediated cell adhesion to a surface (Chesla *et al* 1998). An example plot showing the dependence of adhesion probability (P_a) on the contact duration (t) for different site densities of membrane-bound receptors and immobilized ligands is presented in figure 2. Taking into consideration that the adhesion event is defined as having $n \geqslant 1$ bonds, the dependence of receptor–ligand binding probability on the contact duration time is given by

$$P_a(t) = 1 - P_0(t) = 1 - \exp\left\{-A_c m_r m_l K_a^0 \left[1 - \exp\left(-k_r^0 t\right)\right]\right\}. \quad (5)$$

The 2D binding affinity k_a^0 and the unstressed off-rate k_r^0 can be obtained by a simple graphic representation method, as shown in figure 2. By setting $t \to \infty$ in equation (5), the steady-state solution $P_{a,\mathrm{ss}}$, which represents the maximum adhesion probability for a given set of conditions, is given by

$$P_{a,\mathrm{ss}} = 1 - \exp\left(-A_c m_r m_l K_a^0\right). \quad (6)$$

The 2D affinity constant $A_c K_a^0$ can be estimated directly from the experiment data for a given set of receptor and ligand site densities. The unstressed off-rate k_r^0 can be expressed by (Chesla *et al* 1998)

$$k_r^0 \approx \frac{0.5}{t_{50}}, \quad (7)$$

where t_{50} represents the duration time for $P_a(t)$ to achieve 50% of steady-state value $P_{a,\mathrm{ss}}$ as shown in the figure 2. Although we cannot directly estimate k_f^0, an alternative expression of the on-rate, $A_c k_f^0$, can be obtained by multiplying 2D binding affinity $A_c K_a^0$ with unstressed off-rate k_r^0.

Effects of molecular length and orientation on 2D binding kinetics

Cell adhesion is regulated not only by the intrinsic kinetic and mechanical properties of receptor–ligand pairs but also other geometric factors such as the length and orientation of adhesion molecules. The critical role of the molecular length in receptor–ligand binding kinetics was first demonstrated by rolling PSGL-1-expressing PMNs on different P-selectin constructs whose lengths were engineered by controlling the number of CR domains (Patel *et al* 1995b). P-selectin constructs containing only two or three CR domains failed to support PMN binding in shear flow even though they exhibited a similar binding efficiency as that of native P-selectin under static conditions (Patel *et al* 1995b). The impact of the molecular length on the 2D selectin–ligand binding kinetics was also investigated by the micropipette aspiration assay using two types of soluble P-selectin: P-selectin consisting of Lec-EGF domains plus 9 CR but no transmembrane and cytoplasmic domains, and P-selectin consisting of only the Lec-EGF domains with an added C-terminal epitope. The 2D affinity $A_c K_a^0$ of the long P-selectin molecule is ~twofold larger than that of the short molecule; however, the molecular length did not have an appreciable effect on the unstressed off-rates k_r^0 (Huang *et al* 2004). Cumulatively, these findings suggest that the absence of PMN binding to immobilized P-selectin constructs bearing two or three CR domains (Patel *et al* 1995b) can be attributed to the poor accessibility of the short molecule to the ligand-coated surface. Once P-selectin–ligand bonds form, their dissociation is not altered by the length of the molecules.

The effect of molecular orientation on the 2D binding kinetics was also investigated using the micropipette aspiration assay. Soluble P- or E-selectin was either adsorbed randomly or uniformly coupled to non-blocking anti-P- or E-selectin antibodies, respectively, on the RBC surface. The 2D binding affinity of uniformly oriented selectins is markedly higher than that of randomly absorbed selectins, whereas no difference was noted in their respective unstressed off-rates (Huang *et al* 2004). Taken together, the molecular length and orientation of selectins modulate the 2D selectin–ligand binding affinity without altering the unstressed off-rate.

Receptor–ligand dissociation: slip bond dissociation kinetics

The kinetic and micromechanical properties of receptor–ligand bond dissociation have been studied by the use of single-molecule force spectroscopy. There are two types of ultrasensitive probes: the biomembrane force probe (BFP) where force is sensed by the displacement of a glass microsphere attached to a pressurized membrane capsule (i.e. RBC) (Evans *et al* 2001, 2004), and the molecular force probe (MFP) where force is sensed by the deflection of a thin cantilever (Evans 2001, Hanley *et al* 2003, 2004, Marshall *et al* 2003). Both techniques can quantify the tensile strength of receptor–ligand pairs at the single molecule level, and allow detection of a wide force spectrum ranging from 5 pN to

>1 nN, which covers the typical biological forces from the molecular to the cellular level (Dobrowsky *et al* 2008, Evans *et al* 2001, 2004, Evans and Calderwood 2007, Hanley *et al* 2003, 2004, Marshall *et al* 2003, Sarangapani *et al* 2004, Helenius *et al* 2008, Muller *et al* 2009). In this section, we review the kinetic models of slip bond dissociation used to extract the biophysical properties of receptor–ligand pairs from BFP and MFP experiments. Slip bonds are defined as those whose bond lifetimes decrease with the application of an external force, because force reduces the energy barrier between bound and free states. Of note, all receptor–ligand pairs exhibit the slip bond dissociation kinetics in the high force regime.

When a receptor is in close proximity with a ligand, the bond formation can be described by a reversible bimolecular reaction with two discrete steps: receptor–ligand encounter and reaction. This conceptual design (Bell 1978) is expressed by

$$R + L \underset{d_-}{\overset{d_+}{\rightleftharpoons}} RL \underset{r_-}{\overset{r_+}{\rightleftharpoons}} \text{Bond} \tag{8}$$

where R is a free receptor molecule, L is a free ligand molecule, d_+ and d_- are the rates of formation and dissociation of the encounter complex RL, r_+ and r_- are the forward and reverse rates for the bond formation. In most cases, the concentration of RL complex is significantly lower than that of free receptor R and free ligand L. Consequently, equation (8) can be simplified by assuming each bond is formed directly from the pair of free molecules (Bell 1978). The overall binding process is thus represented by

$$R + L \underset{k_r}{\overset{k_f}{\rightleftharpoons}} \text{Bond} \tag{9}$$

where k_f and k_r are the on- and off-rates of the bond resulting from a free receptor and a free ligand pair. In 1978, Bell proposed the force dependence of receptor–ligand bond dissociation, which is given by

$$k_r(f) = k_r^0 \exp\left[\frac{x_\beta f}{k_B T}\right] \tag{10}$$

where k_r^0 is the unstressed off-rate, x_β is the reactive compliance, f is the rupture force acting on the bond, $k_B T$ is the Boltzmann constant multiplied by the temperature (or thermal energy). The off-rate, k_r, which is related to bond lifetime t_b by $t_b = 1/k_r$, exponentially increases with the applied force. In the literature, k_r is also given in the following form (Merkel *et al* 1999, Evans and Calderwood 2007):

$$k_r(f) = k_r^0 \exp\left[\frac{f}{f_\beta}\right]. \tag{11}$$

The new parameter $f_\beta = k_B T/x_\beta$ has units of force, and can be considered as the characteristic force scale at which the dissociation rate changes 2.7-fold. Equations (10) and (11) are commonly used to model slip bond dissociation under force.

In practice, it is essentially impossible to apply a force instantaneously. Therefore, there is always a finite loading rate r_f. Evans and colleagues (Evans and Ritchie 1997) proposed a model to estimate the dissociation parameters when a bond is ruptured by a finite loading rate. The probability of a single bond rupture in the time interval $(t,\ t + \mathrm{d}t)$ as a function of force is given by (Evans and Ritchie 1997)

$$p(t,\ f) = k_r(f) \exp\left\{-\int_0^t k_r[f(t')]\,\mathrm{d}t'\right\} \tag{12}$$

where the exponential term represents the probability of bond survival up to time t, whereas the $k_r(f)$ term represents the probability of bond rupture in the next short time interval $\mathrm{d}t$. The peak value of this probability distribution can be obtained by taking the derivative of equation (12) with respect to f. By setting $\vartheta p/\vartheta f = 0$ and using the linear ramp of force, $f(t) = r_f \cdot t$, the off-rate at the critical rupture force $\langle f_b \rangle$ is given by

$$k_r(\langle f_b \rangle) = r_f \frac{\partial}{\partial f}[\ln k_r(f)]_{f=\langle f_b \rangle}. \tag{13}$$

This equation suggests that the bond off-rate increases with the loading rate r_f. Substituting the Bell model equation into equation (13) results in equation (14):

$$\langle f_b \rangle = \frac{k_B T}{x_\beta} \ln\left(\frac{x_\beta}{k_r^0 k_B T}\right) + \frac{k_B T}{x_\beta} \ln(r_f). \tag{14}$$

By plotting the rupture force $\langle f_b \rangle$ against the logarithm of loading rate $\ln(r_f)$, the Bell model parameters, k_r^0 and x_β, can be estimated from the slope and intercept of experimental data in the linear region by using the following equations (Merkel *et al* 1999, Tees *et al* 2001, Hanley *et al* 2004):

$$\text{slope}: \frac{k_B T}{x_\beta}; \quad \text{intercept}: \frac{k_B T}{x_\beta} \ln\left(\frac{x_\beta}{k_r^0 k_B T}\right). \tag{15}$$

Alternatively, k_r^0 and x_β can also be estimated by a nonlinear least-squares fit of equation (16) to the experimental data over the entire range of loading rates (Evans and Ritchie 1997, Hanley *et al* 2003, Tees *et al* 2001):

$$\langle f_b \rangle = \frac{k_b T}{x_\beta} \exp\left(\frac{k_r^0 k_b T}{x_\beta r_f}\right) \int_1^\infty \frac{\exp\left(\frac{-k_r^0 k_b T}{x_\beta r_f} t\right)}{t} \mathrm{d}t. \tag{16}$$

The accuracy of the Bell model parameters can be validated by Monte Carlo simulations of receptor–ligand bond rupture under constant loading rates (Hanley *et al* 2003, 2004). In brief, given values for k_r^0 and x_β in each simulation, the rupture force ($F_{\text{rup}} = r_f \times n\Delta t$) at a prescribed loading rate can be calculated for which the probability of bond rupture, P_{rup}, is greater than P_{ran}, a random number between 0 and 1:

$$P_{\text{rup}} = 1 - \exp\left[-k_r^0 \exp\left(\frac{x_\beta r_f n \Delta t}{k_b T}\right) \Delta t\right]. \tag{17}$$

where $n = 1, 2, 3, \ldots$, Δt is the interval and $n\Delta t$ is the time step.

Receptor–ligand dissociation: catch bond dissociation kinetics

The Bell model was proposed to describe the dissociation kinetics of the so-called slip bonds (Bell 1978). Ten years

later, Dembo proposed an alternative model, in which the off-rate increases exponentially with the square of applied force (Dembo *et al* 1988). As a theoretical possibility, Dembo suggested that the bond lifetime may also increase with the applied force or remain unchanged; these bonds were classified as catch and ideal bonds, respectively. Catch binding is an intriguing and counter-intuitive phenomenon in which receptor–ligand bonds resist breakage and become stronger under the influence of a low externally applied force. Application of higher forces is expected to reduce the energy barrier between the bound and free states, and as such receptor–ligand bonds follow the slip dissociation kinetics. To date, at least four distinct receptor–ligand pairs show evidence of catch bond behavior in the low force regime and transition to slip bond dissociation at higher forces: selectin–ligand (Marshall *et al* 2003, Sarangapani *et al* 2004, Yago *et al* 2004), glycoprotein Ib-von Willebrand factor (Yago *et al* 2008), the bacterial adhesion protein FimH-mannose (Thomas *et al* 2002), and integrin–ligand bonds (Kong *et al* 2009). This seemingly paradoxical phenomenon at the nanoscale level translates into complex behavior witnessed at the cellular level, such as shear-threshold phenomenon in which the extent of cell binding to selectins, for instance, first increases and then decreases while monotonically increasing the wall shear stress (Finger *et al* 1996, Lawrence *et al* 1997).

The energy landscape that describes the dissociation of a slip bond has a bound state, which is separated from the free state by a potential energy barrier corresponding to the transition state. According to the Dembo model, the bound state and the transition state of a receptor–ligand bond are Hookean springs with specific elastic constants (k) and resting lengths (λ). If the elastic constant is the same for both springs but the difference between the resting lengths of the transition state and bound state springs, $\delta\lambda$, is positive, the off-rate of the receptor–ligand pair can be expressed as an exponential function of the applied force f (Dembo *et al* 1988), as shown in equation (18). If the resting lengths are the same for both springs but the difference between the elastic constants of the transition state and bound state springs, $\delta\kappa$, is negative, the off-rate increases exponentially as the square of the force (Dembo *et al* 1988):

$$k_r(f) = k_r^0 \exp\left\{\frac{(\delta\lambda)\, f - \frac{\delta k}{2k^2} f^2}{k_B T}\right\}, \tag{18}$$

where k_r is the off-rate in the presence of an applied force f, k_r^0 is the unstressed off-rate and k is the elastic constant of the bound state. To account for the distinctions between slip and catch bonds, the possibilities of $\delta\lambda < 0$ and $\delta\kappa > 0$ were considered. In the latter scenarios, the off-rate decreases exponentially with the applied force or the square of force. It was thought that the application of external force on the catch bond decreases its failure rate in the low force regime, but this scenario switches to the traditional slip binding at higher forces where the applied force increases the failure rate.

Various physical and mathematical models have been proposed to describe the experimentally observed catch and slip bond behavior exhibited by selectin–ligand bonds. Conceptually, the receptor–ligand bond can be thought to be shaped like a harpoon or a hook. This configuration can lock 'tightly' when pulled apart by the two ends. Initially the unbinding time (or bond lifetime) increases with the applied force, indicative of catch bond behavior. Progressively increasing forces are capable of bending the elastic hook, thereby promoting dissociation via the slip pathway (Thomas *et al* 2008b). Alternatively, the receptor can undergo a ligand-induced switch to an active conformation (Thomas *et al* 2008b). The transition state in the catch pathway would reflect reversion to the inactive conformation followed by immediate receptor–ligand unbinding. The slip pathway would involve unbinding through the active conformation, similar to the forceful bending of the elastic hook.

A simple four-parameter model (Pereverzev *et al* 2005) was proposed to describe the unbinding of the selectin–ligand complex from a single bound state either along the catch bond pathway over a low-energy barrier or the slip bond pathway over a high-energy barrier. In the absence of an external force, the transition of the receptor–ligand complex from the bound to the free state is related to the thermal probability of reaching the top of the barrier. However, in the presence of an applied force, f, the height of the energy barrier ΔE changes depending on the distance between the bound state 1 and the transition state 2 projected on to the direction of the externally applied force. When the applied tensile force pulls the bond from the bound state to the transition state by performing positive work on the ligand, the energy barrier is lowered (figure 3). The bond breakage in this case is through a single pathway where the projected distance is positive ($x_{12} > 0$) and the receptor–ligand complex forms a slip bond. But force can also pull the ligand away from the transition state in such a way that the projected distance becomes negative ($x_{12} < 0$). Under this circumstance, the force performs negative work on the ligand, thereby increasing the depth of the energy barrier ΔE and decreasing the off-rate (figure 3). In other words, the applied tensile force increases the lifetime of the receptor–ligand bound complex thereby making it a catch bond (Dembo *et al* 1988, Pereverzev *et al* 2005).

The bound complex can dissociate from the bound state via two alternative paths that can be represented as two finite energy barriers on either side, for a catch–slip transition to occur. The probability that a ligand is still bound to its receptor at a later time $t > 0$, $P(t)$, decreases with time according to equation (19) (Pereverzev *et al* 2005):

$$\frac{\mathrm{d}P}{\mathrm{d}t} = -\left(k_{1c} + k_{1s}\right) P(t), \tag{19}$$

where k_{1c} and k_{1s} are the dissociation rate constants for unbinding through the catch and slip pathways with the coordinates x_c and x_s, respectively. Along the two pathways, the exponential dependence of the dissociation rates on the applied force is given by the following relations:

$$k_{1c} = k_{1c}^0 \exp\left(\frac{x_{1c} f}{k_B T}\right); \tag{20}$$

$$k_{1s} = k_{1s}^0 \exp\left(\frac{x_{1s} f}{k_B T}\right), \tag{21}$$

where k_{1c}^0 and k_{1s}^0 are the unstressed dissociation rates along the catch and slip pathways, respectively. x_{1c} and x_{1s} are given

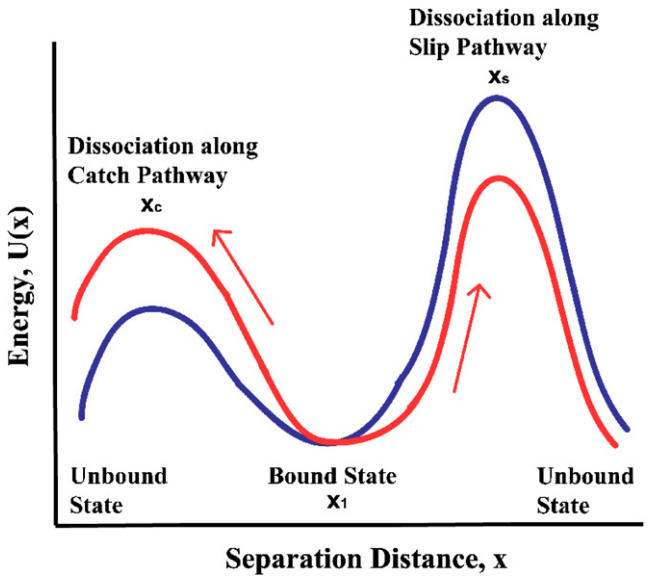

Figure 3. Potential energy landscape for a one state two-pathway dissociation model for catch and slip bonds indicating that the energy barrier along the catch pathway has to be lower than the slip barrier for an efficient catch–slip transition to occur (blue line). The effect of force is depicted by the red line. Modified from Thomas *et al* (2008b).

by $x_{1c} = -\left|\vec{x_c} - \vec{x_1}\right| \cos\theta < 0$; $x_{1s} = \left|\vec{x_s} - \vec{x_1}\right| \cos\theta > 0$ respectively. The solution to the equation for the survival probability is $P(t) = \exp[-(k_{1c} + k_{1s})t]$, which implies that the two-pathway model arising from a single bound state displays a single exponential decay. The inverse mean lifetime of the bound state is given by

$$\frac{1}{\tau(f)} = k_{1c}^0 \exp\left(\frac{x_{1c} f}{k_B T}\right) + k_{1s}^0 \exp\left(\frac{x_{1s} f}{k_B T}\right). \qquad (22)$$

When the applied external force increases from zero, the bond lifetime increases, reaching a maximum value at critical force. Within this force regime, the receptor–ligand bonds exhibit longer lifetimes under force, which is indicative of catch bond behavior. This can be accomplished if k_{1c} decreases more rapidly than k_{1s} increases in the low force regime. However, above the critical force, the slip pathway dominates. A progressive increase in the applied force would accelerate dissociation along the slip pathway by suppressing the energy barrier. Using this model, the four parameters, namely, k_{1c}^0, k_{1s}^0, x_{1c} and x_{1s}, were estimated for previously published experimental P-selectin-PSGL-1 data to be: ${k_{1s}}^0 = 0.25 \pm 0.05\ \mathrm{s}^{-1}$, $x_{1s} = 5.1 \pm 0.5$ Å; ${k_{1c}}^0 = 120 \pm 55\ \mathrm{s}^{-1}$, $x_{1c} = -21.7 \pm 2.4$ Å (Pereverzev *et al* 2005), and found to be in good agreement with MFP data (Hanley *et al* 2004).

Evans and colleagues (Evans *et al* 2004) proposed another two-pathway model, in which the receptor–ligand bond can dissociate along two force-dependent pathways from two bound states that are in thermal equilibrium with each other. A rapid inner conversion between the two states was assumed, which reduced the model parameters from nine to five. The switch from the low impedance pathway (which has a fast dissociation rate) to the high impedance pathway (which has a slow dissociation rate) by the application of an external force is governed by the change in the occupancies of the two bound states, and this determines the transition from catch to slip bond behavior (Evans *et al* 2004). P-selectin-PSGL-1 was found to act as a mechanochemical switch where the force history ascertains the pathway along which the receptor–ligand complex dissociates (Evans *et al* 2004). This hypothesis was tested using a novel jump/ramp mode of force spectroscopy (Evans *et al* 2004).

Experimental demonstration of selectin–ligand catch-to-slip bond transition

The first experimental observation of catch bonds was provided by Zhu and colleagues using force spectroscopy and flow-based adhesion assays (Marshall *et al* 2003). In force spectroscopy experiments, the dimeric form of PSGL-1 or the monomeric recombinant soluble PSGL-1 (sPSGL-1) immobilized on the cantilever was brought repeatedly in contact with P-selectin incorporated into polymer supported lipid bilayers. After applying a constant force to the bond, its lifetime was recorded and plotted as a function of the force producing a characteristic biphasic pattern. In the low force regime, the bond lifetime increased with increasing the force, indicative of the catch bond behavior. Above a critical force level, the bond lifetime decreased with the force, reflective of traditional slip bond behavior. Interestingly, the bond lifetimes and critical force for P-selectin–dimeric PSGL-1 binding were double relative to those for P-selectin-sPSGL-1 binding suggesting that sPSGL-1 forms monomeric bonds with P-selectin, whereas the native form of PSGL-1 forms dimeric bonds with P-selectin (Marshall *et al* 2003). These force spectroscopy observations were validated by the use of flow-based assays. Independent experiments performed by Evans and colleagues (Evans *et al* 2004) using a BFP with a combination of the 'steady ramp' and 'jump/ramp' modes of force spectroscopy also confirmed that P-selectin-PSGL-1 bonds display the catch-to-slip bond transition.

L-selectin binding to its ligands, PSGL-1 and endoglycan, was also found to exhibit catch bond behavior at low forces and transition to slip bond at higher forces (Sarangapani *et al* 2004). In contrast to P-selectin, L-selectin is only capable of making monomeric bonds with PSGL-1 (Sarangapani *et al* 2004).

Both L-selectin and PSGL-1 are expressed on the surface of circulating leukocytes and play a key role in homotypic leukocyte adhesive interactions in shear flow (Jadhav and Konstantopoulos 2002, Taylor *et al* 1996). Without the catch bonds to shorten bond lifetimes in the low shear regime, spontaneous homotypic aggregation of free-flowing leukocytes via an L-selectin-PSGL-1-dependent mechanism would be induced with undesirable clinical manifestations. Catch bonds thus function to prevent leukocyte aggregation when it is not needed (Zhu *et al* 2005).

Estimation of bond dissociation rates from cell rolling assays

In flow-based adhesion assays, the translational velocity at any given instant describes different types of cell motion (Hammer

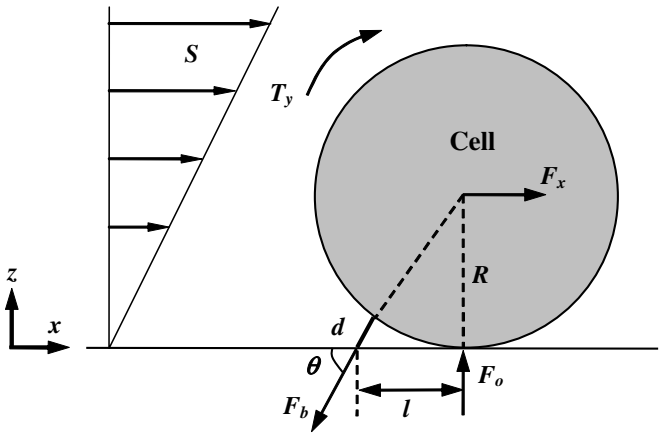

Figure 4. Force balance on a tethered cell in shear flow. A cell of radius R experiences a hydrodynamic force F_x and torque T_y induced by the shear rate S. On the other hand, a tether which has length d and oriented at an angle θ with the substrate induces a force F_b on the cell. The length of lever arm l is the distance between binding points.

and Apte 1992, Chang *et al* 2000, Krasik and Hammer 2004). Specifically, a cell is in free motion when its translational velocity is close to the prevailing hydrodynamic velocity. When the cell mean velocity is significantly slower than the hydrodynamic velocity due to the formation/dissociation of receptor–ligand bonds, the cell is classified as in rolling motion. If a cell is stationary for at least several seconds, it is considered as firmly adherent. Although cell rolling is a complex process controlled by many different physical and chemical parameters, such as cell deformation, microvillus extension, receptor and ligand site densities, and receptor–ligand bond formation and dissociation, several simplifications can still possibly be made. In the low shear regime, the cell deformation can be neglected such that the cell can be modeled as a hard sphere in a Couette flow. The hydrodynamic force and torque exerted on the cell can be determined by $F_x = 1.7 \times (6\pi\mu R^2 S)$ and $T_y = 0.944 \times (4\pi\mu R^3 S)$, respectively (Goldman *et al* 1967), where μ is the viscosity of the suspended buffer, R is the radius of cell and S is the shear rate. If ligands are immobilized on the substrate at very low site densities, the binding interaction can be assumed to involve a single receptor–ligand bond complex. Thus, the bond lifetime can be obtained by simply recording the cell tethering time.

The bond rupture force F_b can be estimated by balancing forces and torques on the cell at static equilibrium, as shown in figure 4. The sum of forces in x- or z-directions must equal zero:

$$F_x = F_b \cos\theta, \tag{23}$$

$$F_o = F_b \sin\theta, \tag{24}$$

where F_o is the contact force between cell and flow chamber in the y-direction. The balance of torque in the y-direction about the contact point of F_o is given by

$$T_y + F_x R = l\,(F_b \sin\theta)\,. \tag{25}$$

The length of the lever arm is equal to the distance between the binding point and the contact point of F_o (figure 4) which can be measured by the distance that bound cells move during flow reversal assays (Chen *et al* 1997, Alon *et al* 1997). The tether length d (figure 4) is the total length of an extended microvillus and the receptor–ligand complex (Alon *et al* 1997, Chen *et al* 1997, Shao *et al* 1998). The oriented angle θ of the tether is expressed by (Shao *et al* 1998)

$$\theta = \tan^{-1}\left(\frac{R}{l}\right) + \cos^{-1}\left(\frac{d^2 + l^2}{2d\sqrt{R^2 + l^2}}\right). \tag{26}$$

To ensure that cell tethering is mediated by a single receptor–ligand pair, flow-based adhesion assays must be performed using a substrate (i.e. chamber wall) coated with very low selectin site densities, typically, lower than those supporting stable cell rolling. The cell tethering time, t_b, represents the bond lifetime. Under a constant force, the dissociation of tethered cells follows the first order kinetics (Alon *et al* 1995b). By plotting the natural logarithm of the number of cells that remained tethered as a function of lifetime, the dissociation rate k_r can be extracted by the negative slope of the fitting curve as shown in figure 5(*a*) (Alon *et al* 1995b, Alon *et al* 1997). By performing the flow chamber assays under different wall shear stresses, the off-rate k_r can be obtained as a function of applied force, which is calculated from equations (23)–(26). The independence of off-rate on the selectin site density on the substrate is indicative of a quantum unit mediating selectin-dependent cell tethering (Alon *et al* 1995b). The kinetic parameters of selectin–ligand bond dissociation can be obtained by fitting the appropriate kinetic model (e.g. two-pathway model (Evans *et al* 2004)) to the off-rate data as a function of force (figure 5(*b*)).

Effects of fluid shear on cell rolling

In the absence of viscous fluid moving around a cell, its translational velocity U_{cell} would be synchronized with the angular velocity Ω when the modeled cell is in the limit of touching the surface. Hence, $R\Omega/U_{\text{cell}}$ would be equal to unity. However, the numerical solutions of $R\Omega/U_{\text{cell}}$ obtained by Goldman *et al* (1967) showed that the value of $R\Omega/U_{\text{cell}}$ approaches a finite limit of $\sim$0.5676 when $z \to R$ (e.g. the modeled cell 'touches' the surface) (figure 4). Consequently, the cell translational velocity U_{cell} is always larger than the surface tangential velocity $R\Omega$, leading to a cell slipping motion relative to the chamber wall. This slipping velocity has been shown to enhance the receptor–ligand encounter rate (Chang and Hammer 1999). In the absence of a slipping motion between the cell surface and the chamber wall, each cell receptor could only interact with a limited number of immobilized counter-receptors located within its reactive zone. In contrast, when a cell surface moves with a finite slipping velocity, each cell receptor can potentially react with any counter-receptor passing its reactive zone. Although fluid shear exerts forces tending to disrupt the receptor–ligand bonds responsible for cell tethering/adhesion, it also induces collisions between free-flowing cells and the vessel wall, thereby increasing the encounter rate between membrane-bound receptors and their ligands (Caputo *et al* 2007, Chang and Hammer 1999). This mechanism potentiates

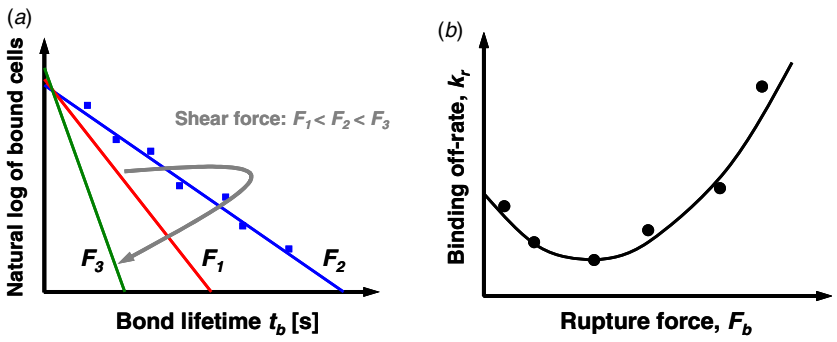

Figure 5. (*a*), Example of distribution of bond lifetimes obtained from cell tethering assays at different shear forces. The receptor–ligand bond off-rate k_r can be estimated from the slope of the logarithm of the number of bound cells versus the bond lifetime (Alon *et al* 1995b). This example plot illustrates that bonds exhibit catch bond behavior at low forces (F_1) and transition to slip bonds at higher forces (F_3). (*b*), Dependence of the off-rate on the rupture force. The catch–slip bond kinetic parameters can be obtained by fitting the appropriate model (e.g. two-pathway model) to the data points (Evans *et al* 2004).

leukocyte attachment to inflamed endothelial cells during the inflammatory response, but can also enhance tumor cell adhesion to vascular endothelium, thereby increasing the risk of tumor cell extravasation to secondary tissues.

Selectin-PSGL-1-dependent interactions require a shear threshold to mediate optimal leukocyte tethering and rolling (Lawrence *et al* 1997, Yago *et al* 2004). In other words, leukocyte tethering rate first increases and then decreases while monotonically increasing wall shear stress. This so-called shear threshold phenomenon seems counter-intuitive because increasing levels of shear stress increase the dissociation force on the bonds, thereby increasing the probability of the cell to detach from the substrate. Both *in vitro* and *in vivo* assays reveal that this phenomenon may be characteristic of all three selectins binding to their respective glycoprotein ligands (Finger *et al* 1996, Lawrence *et al* 1997). Shear-induced cell deformation was initially proposed to explain this phenomenon by increasing the contact area between the cell and the substrate; as such, the probability of bond formation is increased (Lawrence *et al* 1997). However, numerical studies show that cell deformation plays a modest role in the shear threshold phenomenon (Pawar *et al* 2008). In light of observations showing that cell-free flow assays using purified selectins and their respective ligands successfully recapitulate the shear threshold phenomenon (Marshall *et al* 2003, Yago *et al* 2004), it is now accepted that the origin of this phenomenon is primarily molecular, intimately linked with the kinetic and micromechanical properties of receptor–ligand bonds.

Based on the analysis of various biophysical parameters that control selectin-mediated adhesion under flow, Zhu and colleagues identified two major mechanisms that contribute to the shear threshold phenomenon (Zhu *et al* 2008): transport-dependent acceleration of bond formation and force-dependent deceleration of bond dissociation. The first mechanism encompasses three distinct modes of transport (Zhu *et al* 2008): (i) the relative sliding between the cell and the surface; (ii) the Brownian motion, which alters the gap distance between the cell and the surface and increases their collisions; and (iii) the molecular diffusivity of the receptors and ligands, which orients their binding sites for molecular docking. The second mechanism refers to the catch bond kinetics in which the bond lifetime is prolonged by the tether force. Interestingly, simulation studies using the adhesive dynamics model for cell rolling reveal that the shear-threshold phenomenon observed in L-selectin-dependent cell rolling is predominantly attributed to the catch–slip bond kinetics and to a lesser extent to the shear-controlled on rate (Caputo *et al* 2007). Dimensional analysis studies also disclose that the tether force, but not the wall shear rate or wall shear stress, is the critical parameter controlling flow-enhanced cell rolling (Zhu *et al* 2008).

Concluding remarks

The mechanisms used for trafficking of leukocytes may be appropriated for the dissemination of metastatic tumor cells via the bloodstream and lymphatics. In particular, the paradigm of the coordinated action of a 'rapid' selectin-dependent binding followed by a 'slow' integrin-mediated adhesion has been extended to account for maximal binding of tumor cells to activated endothelium (Burdick and Konstantopoulos 2004, Burdick *et al* 2003), platelets (McCarty *et al* 2000, 2002), and PMNs (Jadhav *et al* 2001, Jadhav *et al* 2007, Jadhav and Konstantopoulos 2002) under physiological shear conditions. Significant advances have recently been made in the identification and characterization of functional selectin ligands expressed by metastatic tumor cells (Napier *et al* 2007, Thomas *et al* 2008a), which appear to be distinct from the selectin ligands found on the leukocyte surface. Although the biophysics of selectin-mediated leukocyte binding has been extensively studied, little is known about the biomechanics of selectin–ligand interactions in the context of cancer metastasis (Hanley *et al* 2003). Since these interactions precede and are thus necessary for tumor cell extravasation, and facilitate CTC survival and metastatic outgrowth, a quantitative analysis of selectin–ligand binding will further our understanding of the metastatic process and aid the development of new screening methods and therapeutic strategies that exploit these binding interactions. Elucidating the molecular nature of tumor cell

adhesion in the dynamic setting of the vasculature requires a multidisciplinary approach that integrates fundamentals of hydrodynamics, modeling of receptor–ligand binding kinetics and cell mechanics, with concepts and techniques from biochemistry and molecular and cell biology.

Acknowledgments

This work was supported by NIH/NCI R01 CA101135 and U54 CA143868.

References

Alon R, Chen S, Puri K D, Finger E B and Springer T A 1997 The kinetics of L-selectin tethers and the mechanics of selectin-mediated rolling *J. Cell Biol.* **138** 1169–80

Alon R, Feizi T, Yuen C T, Fuhlbrigge R C and Springer T A 1995a Glycolipid ligands for selectins support leukocyte tethering and rolling under physiologic flow conditions *J. Immunol.* **154** 5356–66

Alon R, Fuhlbrigge R C, Finger E B and Springer T A 1996 Interactions through L-selectin between leukocytes and adherent leukocytes nucleate rolling adhesions on selectins and VCAM-1 in shear flow *J. Cell Biol.* **135** 849–65

Alon R, Hammer D A and Springer T A 1995b Lifetime of the P-selectin-carbohydrate bond and its response to tensile force in hydrodynamic flow *Nature* **374** 539–42

Bell G I 1978 Models for the specific adhesion of cells to cells *Science* **200** 618–27

Borsig L, Wong R, Feramisco J, Nadeau D R, Varki N M and Varki A 2001 Heparin and cancer revisited: mechanistic connections involving platelets, P-selectin, carcinoma mucins, and tumor metastasis *Proc. Natl Acad. Sci. USA* **98** 3352–7

Borsig L, Wong R, Hynes R O, Varki N M and Varki A 2002 Synergistic effects of L- and P-selectin in facilitating tumor metastasis can involve non-mucin ligands and implicate leukocytes as enhancers of metastasis *Proc. Natl Acad. Sci. USA* **99** 2193–8

Burdick M M, Bochner B S, Collins B E, Schnaar R L and Konstantopoulos K 2001 Glycolipids support E-selectin-specific strong cell tethering under flow *Biochem. Biophys. Res. Commun.* **284** 42–9

Burdick M M and Konstantopoulos K 2004 Platelet-induced enhancement of LS174T colon carcinoma and THP-1 monocytoid cell adhesion to vascular endothelium under flow *Am. J. Physiol. Cell Physiol.* **287** C539–47

Burdick M M, Mccaffery J M, Kim Y S, Bochner B S and Konstantopoulos K 2003 Colon carcinoma cell glycolipids, integrins, and other glycoproteins mediate adhesion to HUVECs under flow *Am. J. Physiol. Cell Physiol.* **284** C977–87

Camerer E, Qazi A A, Duong D N, Cornelissen I, Advincula R and Coughlin S R 2004 Platelets, protease-activated receptors, and fibrinogen in hematogenous metastasis *Blood* **104** 397–401

Caputo K E, Lee D, King M R and Hammer D A 2007 Adhesive dynamics simulations of the shear threshold effect for leukocytes *Biophys. J.* **92** 787–97

Chang K C and Hammer D A 1999 The forward rate of binding of surface-tethered reactants: effect of relative motion between two surfaces *Biophys. J.* **76** 1280–92

Chang K C, Tees D F and Hammer D A 2000 The state diagram for cell adhesion under flow: leukocyte rolling and firm adhesion *Proc. Natl Acad. Sci. USA* **97** 11262–7

Chen S, Alon R, Fuhlbrigge R C and Springer T A 1997 Rolling and transient tethering of leukocytes on antibodies reveal specializations of selectins *Proc. Natl Acad. Sci. USA* **94** 3172–7

Chesla S E, Selvaraj P and Zhu C 1998 Measuring two-dimensional receptor–ligand binding kinetics by micropipette *Biophys. J.* **75** 1553–72

Dembo M, Torney D C, Saxman K and Hammer D 1988 The reaction-limited kinetics of membrane-to-surface adhesion and detachment *Proc. R. Soc. Lond. B. Biol.* **234** 55–83

Dobrowsky T M, Panorchan P, Konstantopoulos K and Wirtz D 2008 Live-cell single-molecule force spectroscopy *Methods Cell Biol.* **89** 411–32 chapter 15

Evans E 2001 Probing the relation between force—lifetime—and chemistry in single molecular bonds *Annu. Rev. Biophys. Biomol. Struct.* **30** 105–28

Evans E, Berk D and Leung A 1991 Detachment of agglutinin-bonded red blood cells: I. Forces to rupture molecular-point attachments *Biophys. J.* **59** 838–48

Evans E, Leung A, Hammer D and Simon S 2001 Chemically distinct transition states govern rapid dissociation of single L-selectin bonds under force *Proc. Natl Acad. Sci. USA* **98** 3784–9

Evans E, Leung A, Heinrich V and Zhu C 2004 Mechanical switching and coupling between two dissociation pathways in a P-selectin adhesion bond *Proc. Natl Acad. Sci. USA* **101** 11281–6

Evans E and Ritchie K 1997 Dynamic strength of molecular adhesion bonds *Biophys. J.* **72** 1541–55

Evans E, Ritchie K and Merkel R 1995 Sensitive force technique to probe molecular adhesion and structural linkages at biological interfaces *Biophys. J.* **68** 2580–7

Evans E A and Calderwood D A 2007 Forces and bond dynamics in cell adhesion *Science* **316** 1148–53

Fidler I J, Yano S, Zhang R D, Fujimaki T and Bucana C D 2002 The seed and soil hypothesis: vascularisation and brain metastases *Lancet Oncol.* **3** 53–7

Finger E B, Puri K D, Alon R, Lawrence M B, Von Andrian U H and Springer T A 1996 Adhesion through L-selectin requires a threshold hydrodynamic shear *Nature* **379** 266–9

Frenette P S, Denis C V, Weiss L, Jurk K, Subbarao S, Kehrel B, Hartwig J H, Vestweber D and Wagner D D 2000 P-Selectin glycoprotein ligand 1 (PSGL-1) is expressed on platelets and can mediate platelet–endothelial interactions *in vivo J. Exp. Med.* **191** 1413–22

Gasic G J, Gasic T B and Stewart C C 1968 Antimetastatic effects associated with platelet reduction *Proc. Natl Acad. Sci. USA* **61** 46–52

Goldman A J, Cox R G and Brenner H 1967 Slow viscous motion of a sphere parallel to a plane wall: 2. Couette flow *Chem. Eng. Sci.* **22** 653–60

Hammer D A and Apte S M 1992 Simulation of cell rolling and adhesion on surfaces in shear flow: general results and analysis of selectin-mediated neutrophil adhesion *Biophys. J.* **63** 35–57

Hanley W, McCarty O, Jadhav S, Tseng Y, Wirtz D and Konstantopoulos K 2003 Single molecule characterization of P-selectin/ligand binding *J. Biol. Chem.* **278** 10556–61

Hanley W D, Napier S L, Burdick M M, Schnaar R L, Sackstein R and Konstantopoulos K 2006 Variant isoforms of CD44 are P- and L-selectin ligands on colon carcinoma cells *FASEB J.* **20** 337–9

Hanley W D, Wirtz D and Konstantopoulos K 2004 Distinct kinetic and mechanical properties govern selectin–leukocyte interactions *J. Cell Sci.* **117** 2503–11

Harada N, Mizoi T, Kinouchi M, Hoshi K, Ishii S, Shiiba K, Sasaki I and Matsuno S 2001 Introduction of antisense CD44S CDNA down-regulates expression of overall CD44 isoforms and inhibits tumor growth and metastasis in highly metastatic colon carcinoma cells *Int. J. Cancer* **91** 67–75

Hashino J, Fukuda Y, Oikawa S, Nakazato H and Nakanishi T 1994 Metastatic potential of human colorectal carcinoma SW1222 cells transfected with cDNA encoding carcinoembryonic antigen *Clin. Exp. Metastasis* **12** 324–8

Helenius J, Heisenberg C P, Gaub H E and Muller D J 2008 Single-cell force spectroscopy *J. Cell Sci.* **121** 1785–91
Huang J, Chen J, Chesla S E, Yago T, Mehta P, McEver R P, Zhu C and Long M 2004 Quantifying the effects of molecular orientation and length on two-dimensional receptor–ligand binding kinetics *J. Biol. Chem.* **279** 44915–23
Huang J, Zarnitsyna V I, Liu B, Edwards L J, Jiang N, Evavold B D and Zhu C 2010 The kinetics of two-dimensional TCR and pMHC interactions determine T-cell responsiveness *Nature* **464** 932–6
Jadhav S, Bochner B S and Konstantopoulos K 2001 Hydrodynamic shear regulates the kinetics and receptor specificity of polymorphonuclear leukocyte–colon carcinoma cell adhesive interactions *J. Immunol.* **167** 5986–93
Jadhav S, Eggleton C D and Konstantopoulos K 2005 A 3D computational model predicts that cell deformation affects selectin-mediated leukocyte rolling *Biophys. J.* **88** 96–104
Jadhav S, Eggleton C D and Konstantopoulos K 2007 Mathematical modeling of cell adhesion in shear flow: application to targeted drug delivery in inflammation and cancer metastasis *Curr. Pharmaceutical Des.* **13** 1511–1526
Jadhav S and Konstantopoulos K 2002 Fluid shear- and time-dependent modulation of molecular interactions between polymorphonuclear leukocytes and colon carcinomas *Am. J. Physiol. Cell Physiol.* **283** C1133–43
Kannagi R 1997 Carbohydrate-mediated cell adhesion involved in hematogenous metastasis of cancer *Glycoconj. J.* **14** 577–84
Kansas G S 1996 Selectins and their ligands: current concepts and controversies *Blood* **88** 3259–87
Karpatkin S, Pearlstein E, Ambrogio C and Coller B S 1988 Role of adhesive proteins in platelet tumor interaction in vitro and metastasis formation *in vivo J. Clin. Invest.* **81** 1012–9
Kim Y J, Borsig L, Varki N M and Varki A 1998 P-selectin deficiency attenuates tumor growth and metastasis *Proc. Natl Acad. Sci. USA* **95** 9325–30
Kong F, Garcia A J, Mould A P, Humphries M J and Zhu C 2009 Demonstration of catch bonds between an integrin and its ligand *J Cell Biol.* **185** 1275–84
Konstantopoulos K and Thomas S N 2009 Cancer cells in transit: the vascular interactions of tumor cells *Annu. Rev. Biomed. Eng.* **11** 177–202
Krasik E F and Hammer D A 2004 A semianalytic model of leukocyte rolling *Biophys. J.* **87** 2919–30
Laubli H, Stevenson J L, Varki A, Varki N M and Borsig L 2006 L-selectin facilitation of metastasis involves temporal induction of Fut7-dependent ligands at sites of tumor cell arrest *Cancer Res.* **66** 1536–42
Lawrence M B, Kansas G S, Kunkel E J and Ley K 1997 Threshold levels of fluid shear promote leukocyte adhesion through selectins (CD62L, P, E) *J. Cell Biol.* **136** 717–27
Leppanen A, White S P, Helin J, McEver R P and Cummings R D 2000 Binding of glycosulfopeptides to P-selectin requires stereospecific contributions of individual tyrosine sulfate and sugar residues *J. Biol. Chem.* **275** 39569–78
Long M A, Goldsmith H L, Tees D F J and Zhu C 1999 Probabilistic modeling of shear-induced formation and breakage of doublets cross-linked by receptor–ligand bonds *Biophys. J.* **76** 1112–28
Mannori G, Crottet P, Cecconi O, Hanasaki K, Aruffo A, Nelson R M, Varki A and Bevilacqua M P 1995 Differential colon cancer cell adhesion to E-, P-, and L-selectin: role of mucin-type glycoproteins *Cancer Res.* **55** 4425–31
Mannori G, Santoro D, Carter L, Corless C, Nelson R M and Bevilacqua M P 1997 Inhibition of colon carcinoma cell lung colony formation by a soluble form of E-selectin *Am. J. Pathol.* **151** 233–43
Marshall B T, Long M, Piper J W, Yago T, McEver R P and Zhu C 2003 Direct observation of catch bonds involving cell-adhesion molecules *Nature* **423** 190–3
McCarty O J, Mousa S A, Bray P F and Konstantopoulos K 2000 Immobilized platelets support human colon carcinoma cell tethering, rolling, and firm adhesion under dynamic flow conditions *Blood* **96** 1789–97
McCarty O J T, Jadhav S, Burdick M M, Bell W R and Konstantopoulos K 2002 Fluid shear regulates the kinetics and molecular mechanisms of activation-dependent platelet binding to colon carcinoma cells *Biophys. J.* **83** 836–48
McEver R P and Cummings R D 1997a Perspectives series: cell adhesion in vascular biology. Role of PSGL-1 binding to selectins in leukocyte recruitment *J. Clin. Invest.* **100** 485–91
McEver R P and Cummings R D 1997b Role of PSGL-1 binding to selectins in leukocyte recruitment *J. Clin. Invest.* **100** S97–103
McQuarrie D A, Russell M E and Jachimowicz C J 1964 Kinetics of small systems: II *J. Chem. Phys.* **40** 2914–21
Merkel R, Nassoy P, Leung A, Ritchie K and Evans E 1999 Energy landscapes of receptor–ligand bonds explored with dynamic force spectroscopy *Nature* **397** 50–3
Minami S, Furui J and Kanematsu T 2001 Role of carcinoembryonic antigen in the progression of colon cancer cells that express carbohydrate antigen *Cancer Res.* **61** 2732–5
Muller D J, Helenius J, Alsteens D and Dufrene Y F 2009 Force probing surfaces of living cells to molecular resolution *Nat. Chem. Biol.* **5** 383–90
Napier S L, Healy Z R, Schnaar R L and Konstantopoulos K 2007 Selectin ligand expression regulates the initial vascular interactions of colon carcinoma cells: the roles of CD44v and alternative sialofucosylated selectin ligands *J. Biol. Chem.* **282** 3433–41
Nash G F, Turner L F, Scully M F and Kakkar A K 2002 Platelets and cancer *Lancet Oncol.* **3** 425–30
Nicholson M W, Barclay A N, Singer M S, Rosen S D and Van Der Merwe P A 1998 Affinity and kinetic analysis of L-selectin (CD62L) binding to glycosylation-dependent cell-adhesion molecule-1 *J. Biol. Chem.* **273** 763–70
Nieswandt B, Hafner M, Echtenacher B and Mannel D N 1999 Lysis of tumor cells by natural killer cells in mice is impeded by platelets *Cancer Res.* **59** 1295–300
Nimrichter L *et al* 2008 E-selectin receptors on human leukocytes *Blood* **112** 3744–52
Palumbo J S, Talmage K E, Massari J V, La Jeunesse C M, Flick M J, Kombrinck K W, Jirouskova M and Degen J L 2005 Platelets and fibrin(ogen) increase metastatic potential by impeding natural killer cell-mediated elimination of tumor cells *Blood* **105** 178–85
Park H U, Kim J W, Kim G E, Bae H I, Crawley S C, Yang S C, Gum J R Jr, Batra S K, Rousseau K, Swallow D M, Sleisenger M H and Kim Y S 2003 Aberrant expression of MUC3 and MUC4 membrane-associated mucins and sialyl Le(x) antigen in pancreatic intraepithelial neoplasia *Pancreas* **26** e48-54
Patel K D, Moore K L, Nollert M U and McEver R P 1995a Neutrophils use both shared and distinct mechanisms to adhere to selectins under static and flow conditions *J. Clin. Invest.* **96** 1887–96
Patel K D, Nollert M U and McEver R P 1995b P-selectin must extend a sufficient length from the plasma membrane to mediate rolling of neutrophils *J. Cell Biol.* **131** 1893–902
Pawar P, Jadhav S, Eggleton C D and Konstantopoulos K 2008 Roles of cell and microvillus deformation and receptor–ligand binding kinetics in cell rolling *Am. J. Physiol. Heart Circ. Physiol.* **295** H1439–50
Pereverzev Y V, Prezhdo O V, Forero M, Sokurenko E V and Thomas W E 2005 The two-pathway model for the catch–slip transition in biological adhesion *Biophys. J.* **89** 1446–54
Pinedo H M, Verheul H M, D'amato R J and Folkman J 1998 Involvement of platelets in tumour angiogenesis? *Lancet* **352** 1775–7

Piper J W, Swerlick R A and Zhu C 1998 Determining force dependence of two-dimensional receptor–ligand binding affinity by centrifugation *Biophys. J.* **74** 492–513

Poppe L, Brown G S, Philo J S, Nikrad P V and Shah B H 1997 Conformation of sLe(x) tetrasaccharide, free in solution and bound to E-, P-, and L-selectin *J. Am. Chem. Soc.* **119** 1727–36

Rosen S D 2004 Ligands for L-selectin: homing, inflammation, and beyond *Annu. Rev. Immunol.* **22** 129–56

Sarangapani K K, Yago T, Klopocki A G, Lawrence M B, Fieger C B, Rosen S D, McEver R P and Zhu C 2004 Low force decelerates L-selectin dissociation from P-selectin glycoprotein ligand-1 and endoglycan *J. Biol. Chem.* **279** 2291–8

Satomura Y, Sawabu N, Takemori Y, Ohta H, Watanabe H, Okai T, Watanabe K, Matsuno H and Konishi F 1991 Expression of various sialylated carbohydrate antigens in malignant and nonmalignant pancreatic tissues *Pancreas* **6** 448–58

Shao J Y, Ting-Beall H P and Hochmuth R M 1998 Static and dynamic lengths of neutrophil microvilli *Proc. Natl Acad. Sci. USA* **95** 6797–802

Somasiri A *et al* 2004 Overexpression of the anti-adhesin podocalyxin is an independent predictor of breast cancer progression *Cancer Res.* **64** 5068–73

Somers W S, Tang J, Shaw G D and Camphausen R T 2000 Insights into the molecular basis of leukocyte tethering and rolling revealed by structures of P- and E-selectin bound to SLe(X) and PSGL-1 *Cell* **103** 467–79

Taylor A D, Neelamegham S, Hellums J D, Smith C W and Simon S I 1996 Molecular dynamics of the transition from L-selectin- to beta 2-integrin-dependent neutrophil adhesion under defined hydrodynamic shear *Biophys. J.* **71** 3488–500

Tees D F, Waugh R E and Hammer D A 2001 A microcantilever device to assess the effect of force on the lifetime of selectin–carbohydrate bonds *Biophys. J.* **80** 668–82

Thomas S N, Schnaar R L and Konstantopoulos K 2009a Podocalyxin-like protein is an E-/L-selectin ligand on colon carcinoma cells: comparative biochemical properties of selectin ligands in host and tumor cells *Am. J. Physiol. Cell Physiol.* **296** C505–13

Thomas S N, Tong Z, Stebe K J and Konstantopoulos K 2009b Identification, characterization and utilization of tumor cell selectin ligands in the design of colon cancer diagnostics *Biorheology* **46** 207–25

Thomas S N, Zhu F, Schnaar R L, Alves C S and Konstantopoulos K 2008a Carcinoembryonic antigen and CD44 variant isoforms cooperate to mediate colon carcinoma cell adhesion to E- and L-selectin in shear flow *J. Biol. Chem.* **283** 15647–55

Thomas W E, Trintchina E, Forero M, Vogel V and Sokurenko E V 2002 Bacterial adhesion to target cells enhanced by shear force *Cell* **109** 913–23

Thomas W E, Vogel V and Sokurenko E 2008b Biophysics of catch bonds *Annu. Rev. Biophys.* **37** 399–416

Varki A 1997 Selectin ligands: will the real ones please stand up? *J. Clin. Invest.* **100** S31–5

Walcheck B, Moore K L, McEver R P and Kishimoto T K 1996 Neutrophil–neutrophil interactions under hydrodynamic shear stress involve L-selectin and PSGL-1. A mechanism that amplifies initial leukocyte accumulation on P-selectin *in vitro* *J. Clin. Invest.* **98** 1081–7

Wielenga V J, Heider K H, Offerhaus G J, Adolf G R, Van Den Berg F M, Ponta H, Herrlich P and Pals S T 1993 Expression of CD44 variant proteins in human colorectal cancer is related to tumor progression *Cancer Res.* **53** 4754–6

Yago T *et al* 2008 Platelet glycoprotein Ibalpha forms catch bonds with human WT vWF but not with type 2B von Willebrand disease vWF *J. Clin. Invest.* **118** 3195–207

Yago T, Wu J, Wey C D, Klopocki A G, Zhu C and McEver R P 2004 Catch bonds govern adhesion through L-selectin at threshold shear *J. Cell Biol.* **166** 913–23

Yao L, Pan J, Setiadi H, Patel K D and McEver R P 1996 Interleukin 4 or oncostatin M induces a prolonged increase in P-selectin mRNA and protein in human endothelial cells *J. Exp. Med.* **184** 81–92

Zhu C, Lou J and McEver R P 2005 Catch bonds: physical models, structural bases, biological function and rheological relevance *Biorheology* **42** 443–62

Zhu C, Yago T, Lou J, Zarnitsyna V I and McEver R P 2008 Mechanisms for flow-enhanced cell adhesion *Ann. Biomed. Eng.* **36** 604–21

Zollner O, Lenter M C, Blanks J E, Borges E, Steegmaier M, Zerwes H G and Vestweber D 1997 L-selectin from human, but not from mouse neutrophils binds directly to E-selectin *J. Cell Biol.* **136** 707–16